Microstrip Antenna Phased Array With Electromagnetic Bandgap Substrate

Zeev Iluz, Reuven Shavit, *Senior Member, IEEE*, and Reuven Bauer

***Abstract*—Uniplanar compact electromagnetic bandgap (UC-EBG) substrate has been proven to be an effective measure to reduce surface wave excitation in printed antenna geometries. This paper investigates the performance of a microstrip antenna phased array embedded in an UC-EBG substrate. The results show a reduction in mutual coupling between elements and provide a possible solution to the "blind spots" problem in phased array applications with printed elements. A novel and efficient UC-EBG array configuration is proposed. A probe fed patch antenna phased array of 7×5 elements on a high dielectric constant substrate was designed, built and tested. Simulation and measurement results show improvement in the active return loss and active pattern of the array center element. The tradeoffs used to obtain optimum performance are discussed.**

***Index Terms*—Electromagnetic bandgap (EBG), microstrip antenna phased array, mutual coupling, uniplanar compact electromagnetic bandgap (UC-EBG) geometry.**

I. Introduction

ONE OF THE MAIN problems of phased arrays with wide angular field of view using printed antennas technology is the mutual coupling among elements due to excitation of surface waves in the structure. This effect limits the angular scanning sector and generates in extreme cases blind spots [1]. In the literature, one can find several methods [2] to tackle this problem such as the insertion of conductive fences or vias in between elements to reduce the surface wave coupling between elements. However, these methods have significant drawbacks. These methods disturb the radiation pattern of the element and are costly due to their manufacturing process. Phased arrays antennas based on printed antennas technology encounter two conflicting requirements, on one hand it is desirable to design the radiating elements on low dielectric substrate to obtain high radiation efficiency (avoid excitation of surface waves) and on the other hand it is desirable to utilize high dielectric substrates to obtain a compact integration level of all phased array components. A low cost approach is to design the radiating elements on a high dielectric constant, similar to the rest of the components, and to utilize printed electromagnetic bandgap (EBG) structures to suppress the surface waves excited in such a configuration. The EBG materials offer a unique way to control the excitation of the surface waves in the feeding structure and as such proved to be very effective in reducing the coupling between patch antennas [3]–[5] and improving the overall antenna radiation efficiency.

EBG structures represent a class of periodic structures, which exhibits frequency bandpass and band-stop bands for the surface waves propagating along the structure. Due to this feature they offer the capability to block surface waves excitation in the operational frequency range of the phased arrays. Various EBG structures have been studied extensively in the last decade [3]–[5]. Among the printed EBG configurations, special attention was given to the uniplanar compact electromagnetic bandgap (UC-EBG) [4]. This special configuration is attractive due to its compactness, planarity, low loss and its broad frequency stopband. Another important feature of this configuration is its capability to manifest a complete forbidden bandgap for surface waves in any direction of propagation in the dielectric substrate. Accordingly, this type of EBG was chosen in our phased array study.

In this paper, we present the tradeoffs and design considerations of a probe fed patch antenna phased array of 7×5 elements embedded in a UC-EBG structure printed on a high dielectric substrate. In Section II, a parameter study, for the optimization of the UC-EBG performance in the required frequency bandwidth 4.87–5.84 GHz is described. Next, the required spacing for minimum interaction between the patch antenna and the UC-EBG elements in both E and H planes was studied. In Section III the element design is described. In Section IV the mutual coupling between adjacent elements in both E and H planes is discussed and the impedance and radiation pattern of a center element in a phased array is studied. During this work a comparative study was conducted between the performance of the conventional array (no EBG) to the performance of the same array on a EBG substrate in terms of active impedance and center element active patterns. The tradeoffs made to obtain optimum performance are discussed. A prototype was built and tested and its performance was compared to the computed data obtained using the commercial software MWS from CST, based on a finite-integration time-domain (FITD) algorithm. It is shown that the use of UC-EBG is effective in the reduction of surface waves effect in a printed phased array.

II. EBG Design

The basic EBG element is UC-EBG described in [4] and shown in Fig. 1(a). The unit cell consists of a center metallic square pad loaded with four smaller square pads at each corner. The unit cells are separated by capacitive gaps and interconnected with narrow conductive strips.

Manuscript received January 1, 2003; revised August 6, 2003. This work was supported by ELTA Electronic Industries Ltd., Ashdod, Israel.

Z. Iluz is with the Department of Electrical and Computer Engineering, Ben-Gurion University of the Negev, Beer Sheva 84105, Israel, and also with ELTA Electronic Industries Ltd., Ashdod 77102, Israel.

R. Shavit is with the Department of Electrical and Computer Engineering, Ben-Gurion University of the Negev, Beer Sheva 84105, Israel.

R. Bauer is with ELTA Electronic Industries Ltd., Ashdod 77102, Israel.

Digital Object Identifier 10.1109/TAP.2004.830252

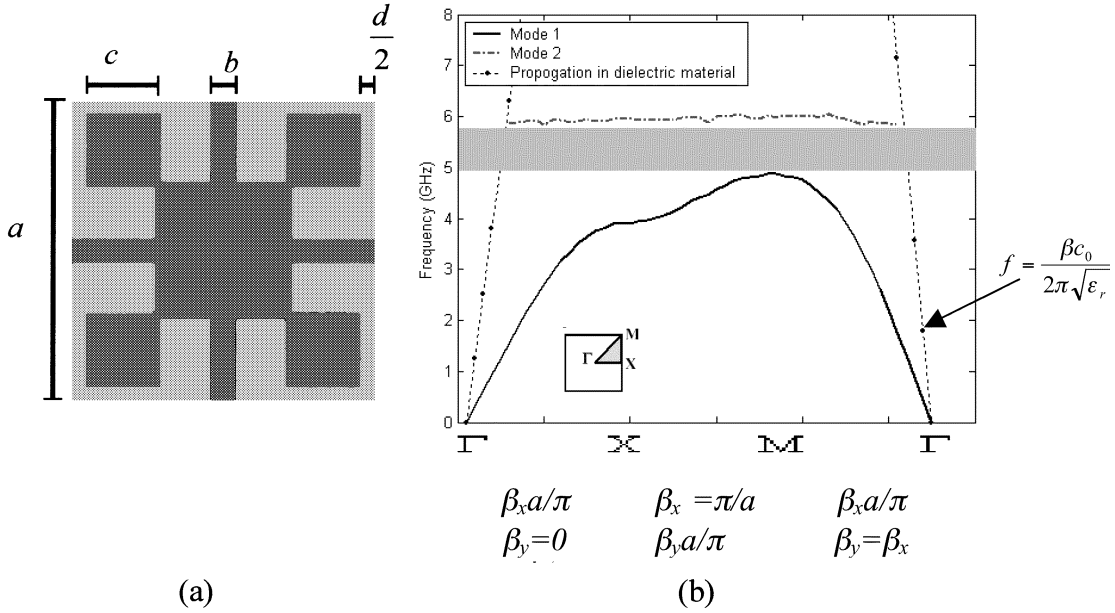

Fig. 1. (a) UC-EBG geometry: a $= 6.6$ mm, b $=$ d $= 0.46$ mm, c $= 1.93$ mm, and $\varepsilon_r = 10.2$. (b) The computed $k-\beta$ dispersion diagram.

The bandgap in [4] was centered at 12.1 GHz and the EBG pattern was printed on a dielectric substrate of 1.27 mm thickness with dielectric constant $\varepsilon_r = 10.2$. To adjust this optimal design to the required new center frequency of 5.75 GHz, the size of the squared UC-EBG unit cell, a was rescaled to 6.6 mm, the substrate thickness was increased to 2.54 mm and the element parameters were optimized to obtain maximum frequency bandstop in all propagation directions. The optimization to the new center frequency was conducted using HFSS a commercial electromagnetic simulator from Ansoft, based on FEM algorithm [6]. Fig. 1(b), shows the $k-\beta$ dispersion diagram of the surface modes propagating in the structure. The first (dominant) surface mode is TM_0, which has no cutoff frequency and the second surface wave mode is TE_1. One can observe a complete stopband between the first mode, TM_0 and the second mode, TE_1 in the frequency band 4.87–5.84 GHz. This stopband is unique to EBG structures, while for a standard dielectric no such stopband exists. The straight dotted lines represent propagation in a dielectric medium with $\varepsilon_r = 10.2$. The $\Gamma - \mathrm{X}$ branch represents $\beta_x \alpha/\pi$with $\beta_y = 0$. The X-M branch represents $\beta_y \alpha/\pi$ with $\beta_x = \pi/\alpha$ and $\mathrm{M} - \Gamma$ branch represents $\beta_x \alpha/\pi$ with $\beta_x = \beta_y$.

III. Radiating Patch Element Design

The basic geometry of the proposed radiating patch element is shown in Fig. 2. The patch is circular with radius R_1 and is printed on a substrate with dielectric constant$\varepsilon_r = 10.2$ and thickness $h = 2.54$ mm. This choice of circular patch geometry in comparison with rectangular patch geometry was made to reduce the element dimensions. The patch is fed by a top loaded pin coupled through an annular gap (inner radius R_2 and outer radius R_3) to the patch as suggested in [7]. This unique type of feeding is necessary in the current circumstance in order to introduce a capacitive effect to counterbalance the excessive inductive effect of the feeding pin, which is electrically long as a result of the relative high thickness of the substrate and its high dielectric constant. The matching optimization was conducted with MWS software from CST. The printed antenna was designed to work at the center frequency 5.75 GHz.

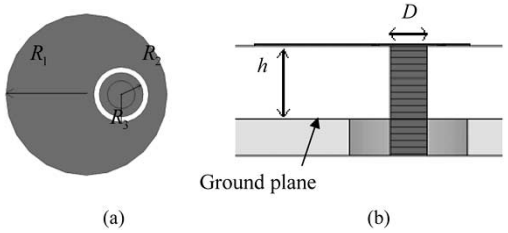

Fig. 2. (a) Top view of the patch: $\mathrm{R}_1 = 3.734$ mm, $\mathrm{R}_2 = 1.016$ mm, $\mathrm{R}_3 = 1.27$ mm. (b) Side view: h $= 2.54$ mm with $\varepsilon_r = 10.2$, D $= 1.3$ mm.

One of the main tradeoff issues in the design of a printed phased array embedded in a UC-EBG periodic structure is the gap, W between the radiating patch and the UC-EBG lattice. A parameter study was conducted to determine the dependence of S_{11} on the variation of W. Fig. 3 presents simulation results of $|S_{11}|$ versus frequency with W as parameter.

One can observe that an increase in the gap width, W reduces the coupling between the UC-EBG and the patch element. This effect can be explained by a reduced near field interaction between the patch and the EBG elements (designed only to absorb surface waves), as w increases. From Fig. 3 it is seen that the optimum gap must be larger then the EBG unit cell, $a = 6.6$ mm in order to have a minimal effect on the resonant frequency, therefore a compromise value of $1.2\,a$ ($W = 7.92$ mm) was chosen for our array configuration. The price paid for increasing the gap is a decrease in the available spacing between the radiating patch elements to insert UC-EBG elements in an array configuration (lower surface wave suppression). An additional parameter study was conducted to determine the angular dependence of the excited surface wave by the radiating patch without the EBG presence. Fig. 4 shows the dependence of the coupling co-

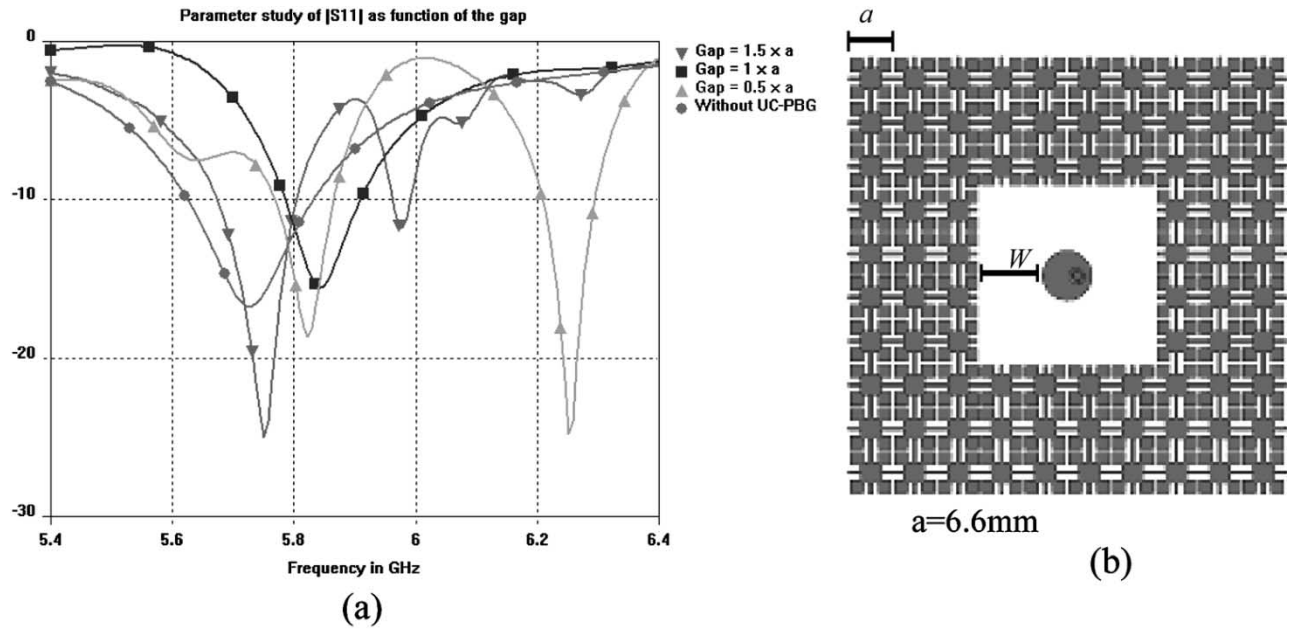

Fig. 3. (a) Simulation results of $|S_{11}|$ versus frequency as a function of the gap width, W. (b) Top view of the patch with the gap, W between the patch and the UC-EBG.

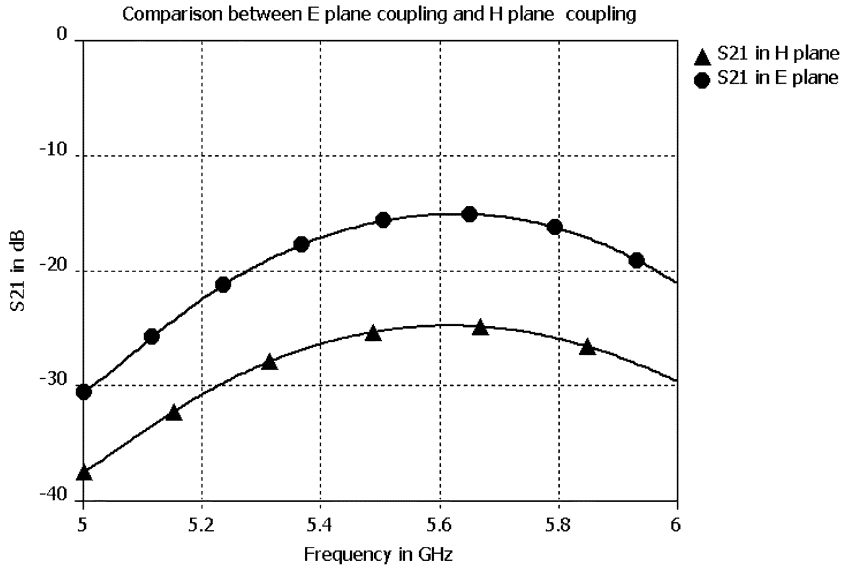

Fig. 4. Simulation results of the coupling coefficient, S_{21} between two patches separated 33.02 mm $(0.63\lambda_0)$ in both E and H planes.

efficient, S_{21} on frequency between two patches separated 33.02 mm ($0.63\lambda_0$ at the operating frequency) in both E and H planes.

One can observe that at the operating frequency the coupling between the patches in the E plane is higher by 10 dB compared to that in the H plane. This result can be primarily attributed to reduction of surface waves excited in the H plane. Moreover, this conclusion triggered the idea to use EBG elements only in the E plane in an array configuration.

IV. Antenna Array Design

The performance of a large phased array with rectangular lattice and inter-element spacings d_x and d_y is mainly characterized by two principal parameters, the active element pattern and the active impedance [8]. Both parameters are dependent on the mutual coupling from all elements in the array to the element under consideration. However, only the close-in elements to this element have a major effect, since the mutual coupling decreases with distance. This finding was systematically investigated in [9] and it has been shown that it is enough to investigate the active element pattern and the active impedance of the center element in a small array (sizes ranging from 25–50 elements) to provide sufficient information on the radiation characteristics of an element in a large phased array. The objective in this study was to determine the EBG effect in a large phased array, however for practical reasons a finite array was considered for both simulations and measurements verification. The center element in the finite array was chosen as the performance

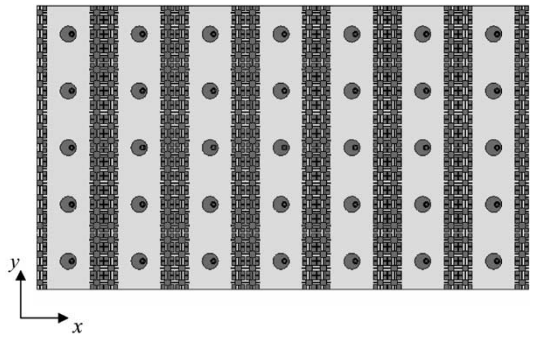

Fig. 5. Top view of the array with the UC-EBG substrate.

indicator of an element in a large phased array. The central element active reflection coefficient, $S_{11}^a(u,v)$ in a finite array with $(2N_x+1)\times(2N_y+1)$ elements was computed by

$$S_{11}^a(u,v) = S_{11}(u,v) + \sum_{m=-N_x}^{N_x}{}' \sum_{n=-N_y}^{N_y}{}' S_{21}(m,n)\exp \times \left[-jnd_x\frac{2\pi}{\lambda}u - jmd_y\frac{2\pi}{\lambda}v\right] \quad (1)$$

in which $\sum'\sum'$ denotes summation on all elements except $\mathrm{m}=\mathrm{n}=0$, $S_{11}(u,v)$ is the self-reflection coefficient of the central element and $S_{21}(m,n)$ is the mutual coupling scattering parameter from the central element to the (m,n) element. The $S_{21}(m,n)$ scattering parameters are summed with the proper phase to obtain the peak beam in the direction (θ_0,ϕ_0). The active reflection parameter $|S_{11}^a|$ is usually presented in $u-v$ plane $(u=\sin\theta_0\cos\phi_0, v=\sin\theta_0\sin\phi_0)$. The parameters $S_{21}(m,n)$ were computed and measured with the center element in the array excited and all other elements terminated.

Based on the investigation in [9], a 7×5 array was chosen as a test case for the large phased array performance. The center frequency of the array is 5.75 GHz. Since the surface wave excitation by the radiating patches is significantly higher in E plane (x axis) compared to H plane (y axis) as concluded from simulation results presented in Fig. 4, it was decided to use UC-EBG elements only in x direction as shown in Fig. 5. This choice enabled us to keep the spacing in y direction to a minimum of $0.506\,\lambda_0$ ($d_y=26.42$ mm), which is optimal for full scanning in H plane upper hemisphere without generating grating lobes in the visible space. The spacing in x direction was chosen as $0.63\lambda_0$ ($d_x=33.02$ mm).

This choice was determined by practical considerations such as: the minimum gap required in E plane between the patch and the UC-EBG elements, the minimum number of UC-EBG cells to obtain suppression of surface waves and the max. field of view in E plane (no grating lobes in the visible range). The chosen spacing d_x, allows insertion of 2 unit cells of UC-EBG between adjacent patch elements as shown in Fig. 5. Previous investigations [10] have shown that two unit cells is the minimum number of cells required to achieve the surface wave suppression phenomena of the EBG. Moreover, the EBG element columns behave similar to an absorbing interface for the surface waves propagating in an angular sector around x axis, as such the effect on the surface waves is more significant compared to the effect obtained by a standard one dimensional inhibitor like conductive fences or vias.

A prototype of the array with and without UC-EBG was manufactured and is displayed in Fig. 6. The performance of this array in terms of its center element active reflection coefficient and active pattern was measured at its center frequency.

Initially, the effectiveness of the UC-EBG to suppress mutual coupling caused by surface waves in the substrate was studied by considering the scattering parameter $|S_{21}|$ of the center element relative to adjacent elements in both E and H planes with and without UC-EBG. The measured data is shown in Table I.

One can observe that the center element in both arrays (with and w/o UC-EBG) is matched ($|S_{11}|=-12$ dB), an indication that the chosen gap between the radiating patch and the EBG structure is large enough. Moreover, it can be noticed that the mutual coupling is significantly higher in E plane than in the H plane due to the radiation mechanism of the patch, which favors surface waves excitation in the E plane. It can be noticed that the $|S_{21}|$ in E plane was reduced in the array with UC-EBG compared to the case without UC-EBG. The results in H plane indicate that $|S_{21}|$ increases in the array with the UC-EBG for the first element, but decreases for the second adjacent element and outward.

Fig. 7, shows the comparison of the measurement and simulation results of the active reflection coefficient $|S_{11}^a|$ for the array without UC-EBG, while Fig. 8 shows the same comparison for the array with UC-EBG.

The active $|S_{11}^a|$ is presented in u − v plane ($u=\sin\theta_0\cos\phi_0, v=\sin\theta_0\sin\phi_0$). Apart from a small shift in the center frequency 5.75 GHz versus 5.44 GHz in the case of no UC-EBG and 5.75 GHz versus 5.56 GHz in the case with UC-EBG, there is a good agreement between simulation and measurement results. Based on Fig. 7, one can observe that for a -10 dB return loss criterion of the active reflection coefficient the available field of view without UC-EBG (simulation) is $-0.36\le v\le 0.36$ for all u, corresponding to E plane scanning angular sector of $-21^\circ\le\theta\le21^\circ$ and no field of view limitation in H plane. In the measured results, the v range is $-0.39\le v\le0.39$ for all u, corresponding to E plane scanning angular sector of $-23^\circ\le\theta\le23^\circ$ and no limitation in H plane. In the case with UC-EBG as shown in Fig. 8, it is observed an improvement in the field of view (simulation) to $-0.54\le v\le0.54$ for all u, corresponding to E plane scanning angular sector of $-33^\circ\le\theta\le33^\circ$ and no field of view limitation in H plane. The corresponding measured results are $-0.59\le v\le0.59$ for all u, corresponding to E plane scanning angular sector of $-36^\circ\le\theta\le36^\circ$ and no limitation in H plane. This improvement can be attributed to the suppression of the surface waves in the case of the array with UC-EBG. Close inspection of the measured and simulated results show a non perfect agreement, especially around $u\approx-0.25$, where the measured results show a much larger field of view compared to the simulated results. A possible justification to the nonperfect agreement between simulation and measurement results of the active reflection coefficient is the different edge effect of the diffracted surface waves caused by different ground plane dimensions, 240×140 mm in simulation compared to 300×220 mm in the measured prototype. This difference in

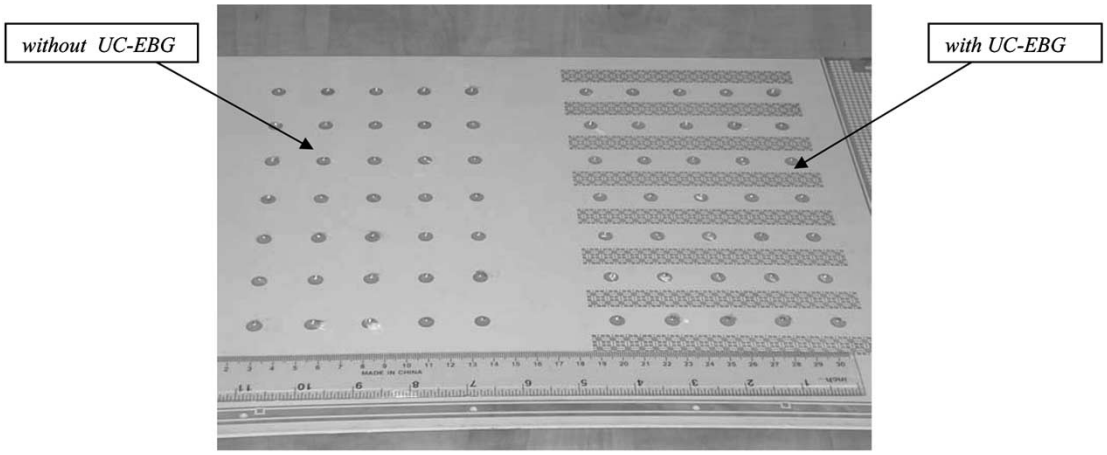

Fig. 6. Layout of the manufactured 7 × 5 printed array with and without UC-EBG.

TABLE I
MEASURED SCATTERING PARAMETER, $|S_{21}|$ OF THE CENTER ELEMENT (AT 5.75 GHz)

Array with UC-EBG	Array w/o UC-EBG	E plane
-12	-12	|S11| in dB (center element)
-18.7	-12.6	$\|S_{21}(1,0)\|$ in dB (to first adjacent element)
-42.8	-24.5	$\|S_{21}(2,0)\|$ in dB (to second adjacent element)
-62	-26.7	$\|S_{21}(3,0)\|$ in dB (to third adjacent element)

Array with UC-EBG	Array w/o UC-EBG	H plane
-12	-12	|S11| in dB (center element)
-15.8	-25.7	$\|S_{21}(0,1)\|$ in dB (to first adjacent element)
-43.6	-27.4	$\|S_{21}(0,2)\|$ in dB (to second adjacent element)

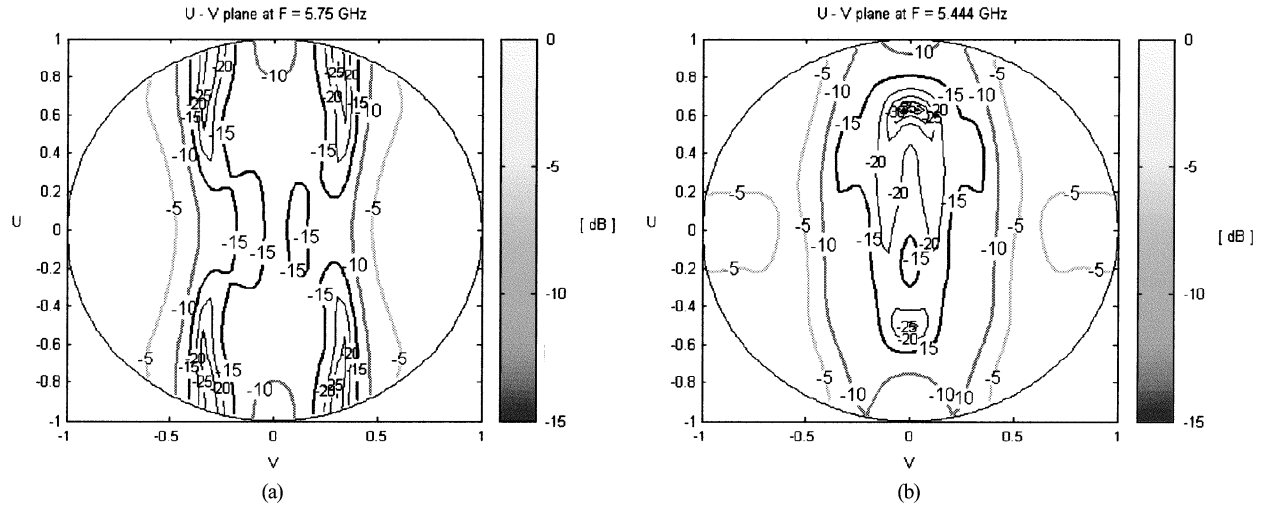

Fig. 7. (a) Simulated and (b) measured active reflection coefficient, $S_{11}^{a}(\mathrm{dB})$ of the center element in a 7 × 5 microstrip array without the UC-EBG.

dimensions was due to some practical considerations of the manufacturing process.

An additional way to test the effectiveness of the UC-EBG on the surface waves behavior in the array is to study the active element pattern of the array. The gain of a fully excited array at a given scan angle is proportional to the active element pattern at this angle. The active element pattern of the center element in the E plane with and without UC-EBG (simulation versus measurement) is shown in Fig. 9. The patterns are plotted for the same frequencies as those of the active reflection coefficient presented in Figs. 7 and 8. The pattern with the UC-EBG is smoother and without the ripples apparent in the case of no UC-EBG.

At $\theta = \pm 30^{\circ}$ one can observe significant nulls (blind spots) in the radiation pattern of the element without UC-EBG. These nulls can be attributed to the diffraction of the excited surface

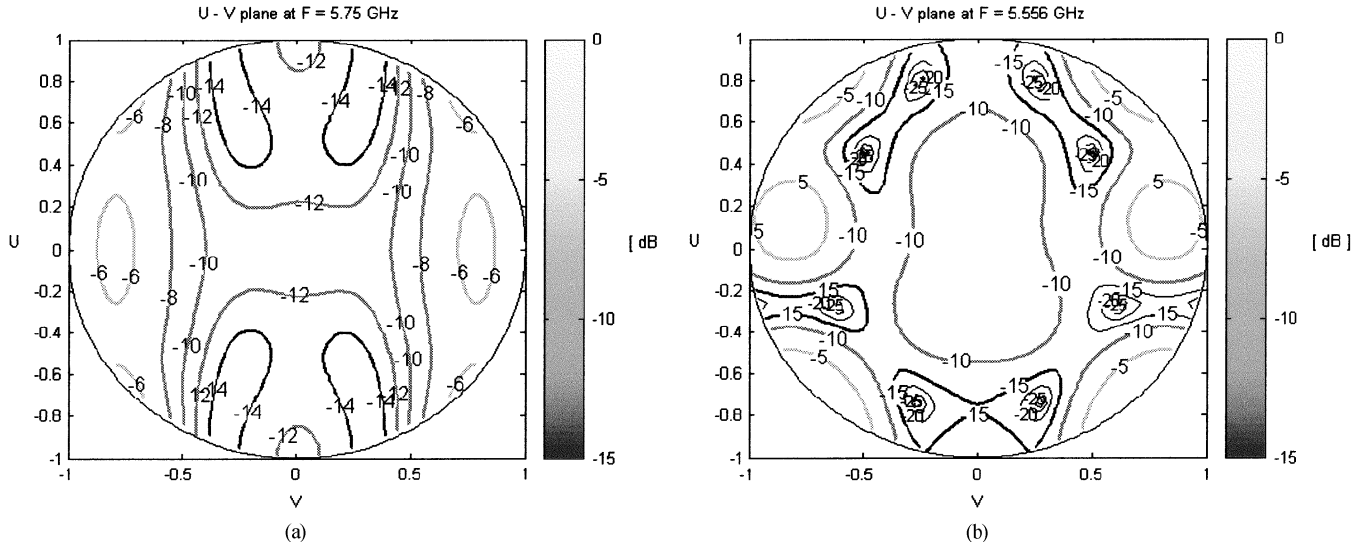

Fig. 8. (a) Simulated and (b) measured active reflection coefficient, $S_{11}^{a}(\mathrm{dB})$ of the center element in a 7×5 microstrip array with the UC-EBG.

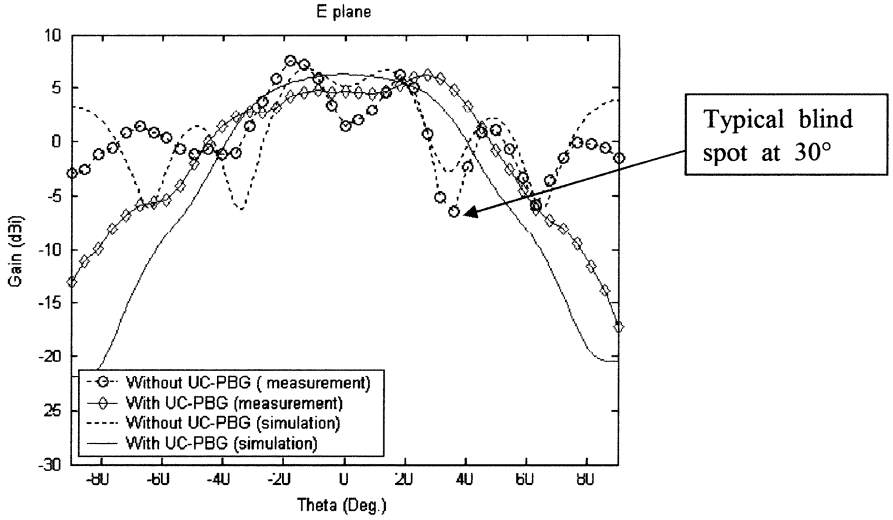

Fig. 9. Simulated and measured active E-plane radiation patterns of the center element with and without the UC-EBG.

waves incident on the array edges, which add out of phase with the main radiation from the center element patch. Moreover, the radiated field amplitude at $\pm 90°$ is lower by 15 dB for the prototype with UC-EBG, which is an indication for the suppression of the surface waves in this case.

The discrepancy between simulation and measured results in the case of the element without UC-EBG may be attributed, as discussed previously, to a different edge effect (different ground plane dimensions) of the diffracted surface waves in simulation and measurement.

The active element pattern in the H plane is shown in Fig. 10 (simulation versus measurement).

In this case, there is almost no major difference between the patterns. This expected result is due to the fact that almost no surface waves are excited in the H plane even without UC-EBG. The agreement between measurement and simulation in this case is better, since the edge effect on the reflected surface waves is negligible.

To fully assess the improvement in the array performance with the UC-EBG the full array gain pattern was computed

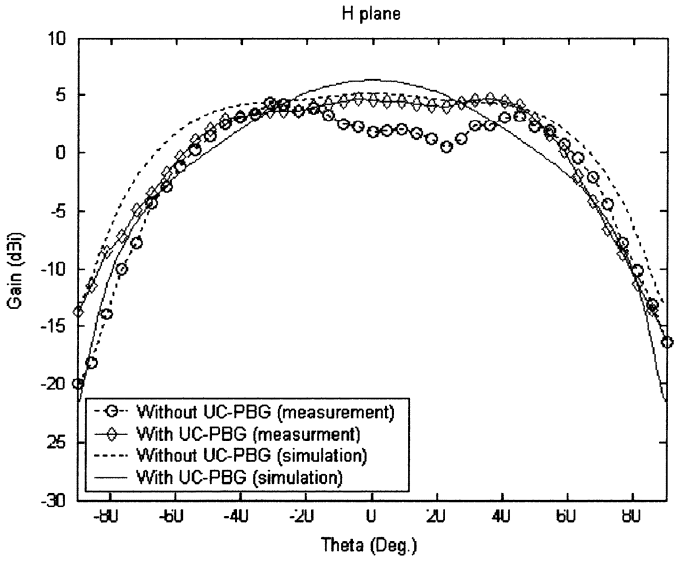

Fig. 10. Simulated and measured active H plane radiation patterns of the center element with and without the UC-EBG.

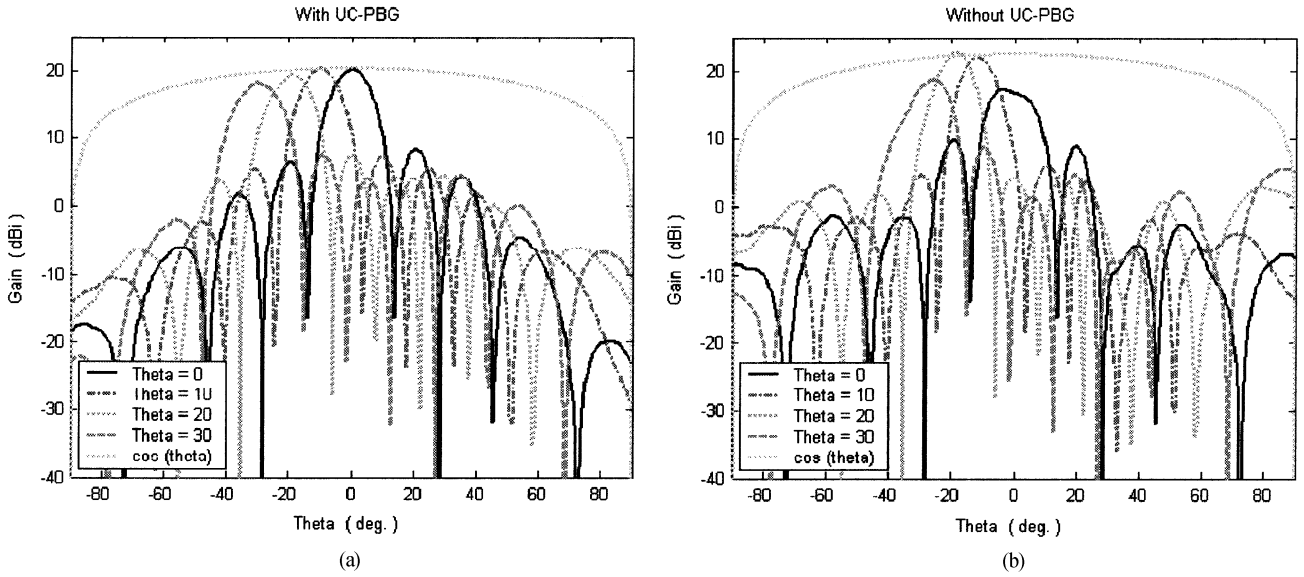

Fig. 11. Simulated gain pattern of a fully excited array in E plane ($\phi = 0°$) for $\theta_{\max} = 0°, 10°, 20°, 30°$, (a) with UC-EBG and (b) without UC-EBG.

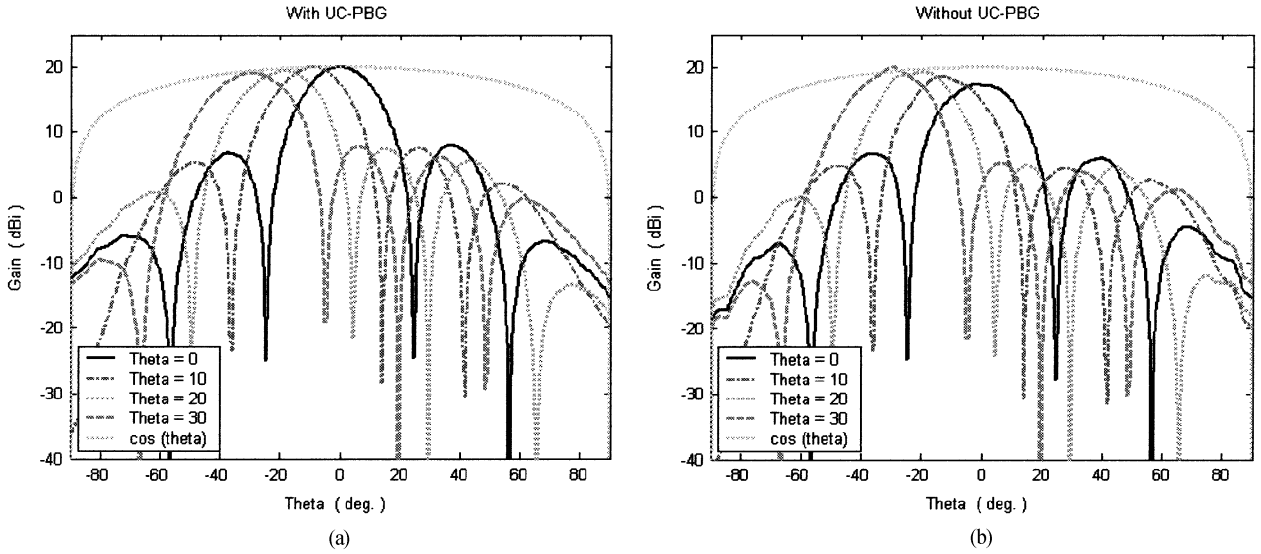

Fig. 12. Simulated gain pattern of a fully excited array in H plane ($\phi = 90°$) for $\theta_{\max} = 0°, 10°, 20°, 30°$, (a) with UC-EBG and (b) without UC-EBG.

for different scan angles (θ_0, ϕ_0). These plots were calculated by multiplying the measured active element pattern shown in Figs. 9 and 10 with the array factor, $A(\theta, \phi)$ given by

$$A(\theta,\phi) = \sum_{m=-N_x}^{N_x} \sum_{n=-N_y}^{N_y} \exp[jkmd_x(\sin\theta\cos\phi - \sin\theta_0\cos\phi_0) + jknd_y(\sin\theta\sin\phi - \sin\theta_0\sin\phi_0)] \quad (2)$$

with $k = 2\pi/\lambda$. Fig. 11 shows the E plane simulated array patterns based on the measured active element pattern for different scan angles, θ_0 ($0°, 10°, 20°$, and $30°$) with and without UC-EBG.

For reference purposes an artificial $\cos\theta$ element pattern was plotted. One can observe that in the case of the array with UC-EBG, the beam peaks follow this element pattern nicely, while the patterns of the array without UC-EBG deviate due to a defected element pattern caused by excessive excitation of surface waves. Moreover, the null (blind spot) that appears at $\pm 30°$ in the element pattern without the UC-EBG is smoothed out and as such increases the ability of the array to scan wider angular sectors. Fig. 12 shows the H plane simulated array patterns based on the measured active element pattern for different scan angles, θ_0 ($0°, 10°, 20°$, and $30°$) with and without UC-EBG. In this case the difference between the array pattern with and without UC-EBG is marginal. This result justifies the decision made not to use UC-EBG in y direction.

V. Conclusion

The performance of a probe fed patch antenna phased array of 7×5 elements embedded in a UC-EBG substrate was investigated as an indicator for the performance of large phased arrays. The simulation and measurement results have shown that the UC-EBG substrate is effective in reducing the mutual coupling

among the patch elements in a phased array configuration. The array performance with UC-EBG was improved in terms of the active return loss (wider scan angles) and active pattern of the center element (elimination of blind spots), by using only two unit cells between adjacent elements. A novel UC-EBG configuration with elements, which affect mainly the phased array E plane radiation pattern was proposed and proved to be effective. Further research is needed to increase the field of view in E plane to much further wider scan angle. This can be accomplished by either using higher dielectric constant substrates or utilizing smaller unit cell EBG structures.

ACKNOWLEDGMENT

The authors wish to thank Dr. C. Samson from ELTA Electronic Industries Ltd., Ashdod, Israel for his continued support throughout all phases of this project.

REFERENCES

[1] D. M. Pozar and D. H. Schaubert, "Analysis of an infinite array of rectangular microstrip patches with idealized probes feeds," *IEEE Trans. Antennas Propagat.*, vol. AP-32, pp. 1101–1107, 1984.

[2] R. J. Mailloux, *Phased Array Antenna Handbook*. Dedham, MA: Artech House, 1993.

[3] Y. Qian, R. Coccioli, D. Sienvenpiper, V. Radisic, E. Yablonovitch, and T. Itoh, "Microstrip patch antenna using novel photonic band-gap structures," *Microwave J.*, vol. 42, no. 1, pp. 66–76, Jan. 1999.

[4] R. Coccioli, F. R. Yang, K. P. Ma, and T. Itoh, "Aperture-coupled patch antenna on UC-PBG substrate," *IEEE Trans. Microwave Theory Tech.*, vol. 47, pp. 2123–2130, Nov. 1999.

[5] P. Maagt, R. Gonzalo, and M. Sorolla, "Enhanced patch antenna performance by suppressing surface wave using PBG substrate," *IEEE Trans. Microwave Theory Tech.*, vol. 47, pp. 2131–2138, Nov. 1999.

[6] R. Remski, "Analysis of PBG surfaces using Ansoft HFSS," *Microwave J.*, vol. 43, no. 1, pp. 51–58, Sept. 2000.

[7] P. S. Hall, "Probe compensation in thick microstrip patches," *Electron. Lett.*, vol. 23, pp. 606–607, Oct. 1987.

[8] D. M. Pozar, "The active element pattern," *IEEE Trans. Antennas Propagat.*, vol. 42, pp. 1176–1178, Aug. 1994.

[9] B. L. Diamond, "Small arrays—Their analysis and their use for the design of array elements," in *Phased Array Antennas*, A. A. Oliner and G. H. Knittel, Eds. Norwood, MA: Artech House, 1972, pp. 127–131.

[10] R. Gonzalo, G. Nagore, I. Ederra, B. Martinez, H. P. M. Pellemans, P. H. Boliver, and P. Maagt, "Coupling between patch antennas on photonic crystals," in *Proc. 24th ESTEC Antenna Workshop*, Noordwijk, The Netherlands, May 30–June 1 2001, pp. 6–10.

Zeev Iluz received the B.Sc. degree in electrical and computer engineering from the Ben-Gurion University of the Negev, Beer-Sheva, Israel, in 2001, where he is working toward the M.Sc. degree in electrical and computer engineering. His thesis involves integration of phased array and electromagnetic bandgap structures.

In 2003, he joined ELTA Electronic Industries Ltd., Ashdod, Israel, where he is working on the development of phased array antennas.

Reuven Shavit (M'82–SM'90) was born in Romania on November 14, 1949. He received the B.S. and M.S. degrees in electrical engineering from the Technion—Israel Institute of Technology, Tel Aviv, in 1971 and 1977, respectively, and the Ph.D. degree in electrical engineering from the University of California, Los Angeles, in 1982.

From 1971 to 1993, he worked as a Staff Engineer and Antenna Group Leader in the Electronic Research Laboratories of the Israeli Ministry of Defense, Tel Aviv, where he was involved in the design of reflector, microstrip, and slot antenna arrays. He was also a part-time Lecturer at Tel Aviv University, teaching various antenna and electromagnetic courses. From 1988 to 1990, he was associated with ESSCO, Concord, MA, as a Principal Engineer involved in scattering analysis and tuning techniques of high performance ground based radomes. Currently, he is with Ben-Gurion University of the Negev, Beer-Sheva, Israel, as a Senior Lecturer doing research in microwave components and antennas. His present research interest is in the areas of tuning techniques for radomes and numerical methods for design microstrip, slot and reflector antennas.

Reuven Bauer received the B.S.E.E. degree from the City College of New York, in 1983 and the M.S.E.E. degree from Northeastern University, Boston, MA, in 1987.

From 1983 to 1985, he was employed at GTE Government Systems, Westborough, MA. From 1985 to 1991, he worked at Raytheon Equipment Division, Wayland, MA. Since 1991, he has been at ELTA Electronic Industries, Ashdod, Israel, working in the Antenna Department, where his primary interests are the development of phased array and microstrip antennas.